frontiers in Chemistry

ORIGINAL RESEARCH
published: 14 July 2021
doi: 10.3389/fchem.2021.712960

CO_2 Activation Within a Superalkali-Doped Fullerene

Giovanni Meloni[1,2]*, *Andrea Giustini*[2] *and Heejune Park*[1]

[1]Department of Chemistry, University of San Francisco, San Francisco, CA, United States, [2]Department of Physical and Chemical Sciences, Università degli Studi de L'Aquila, L'Aquila, Italy

With the aim of finding a suitable synthesizable superalkali species, using the B3LYP/6-31G* density functional level of theory we provide results for the interaction between the buckminsterfullerene C_{60} and the superalkali Li_3F_2. We show that this endofullerene is stable and provides a closed environment in which the superalkali can exist and interact with CO_2. It is worthwhile to mention that the optimized Li_3F_2 structure inside C_{60} is not the most stable C_{2v} isomer found for the "free" superalkali but the D_{3h} geometry. The binding energy at 0 K between C_{60} and Li_3F_2 (D_{3h}) is computed to be 119 kJ mol^{-1}. Once CO_2 is introduced in the endofullerene, it is activated, and the $\widehat{OCO}$ angle is bent to 132°. This activation does not follow the previously studied CO_2 reduction by an electron transfer process from the superalkali, but it is rather an actual reaction where a F (from Li_3F_2) atom is bonded to the CO_2. From a thermodynamic analysis, both CO_2 and the encapsulated [Li_3F_2·CO_2] are destabilized in C_{60} with solvation energies at 0 K of 147 and < −965 kJ mol^{-1}, respectively.

Keywords: CO_2 activation, superalkali, endofullerene, ionization energy, solvation energy

OPEN ACCESS

Edited by:
Ambrish Kumar Srivastava, Deen Dayal Upadhyay Gorakhpur University, India

Reviewed by:
Gourhari Jana, Indian Institute of Technology Bombay, India
Amlan Kusum Roy, Indian Institute of Science Education and Research Kolkata, India

***Correspondence:**
Giovanni Meloni
gmeloni@usfca.edu

Specialty section:
This article was submitted to Theoretical and Computational Chemistry, a section of the journal Frontiers in Chemistry

Received: *21 May 2021*
Accepted: *28 June 2021*
Published: *14 July 2021*

Citation:
Meloni G, Giustini A and Park H (2021) CO_2 Activation Within a Superalkali-Doped Fullerene. Front. Chem. 9:712960. doi: 10.3389/fchem.2021.712960

INTRODUCTION

In 1985, Kroto and co-workers discovered an extremely stable cluster consisting of 60 carbon atoms during a study of long-chain carbon molecules. (Kroto et al., 1985). This cluster, called fullerene, has a football shape with 12 pentagonal and 20 hexagonal rings. (Kroto et al., 1985). Shortly after, a study presenting successful formation of fullerenes with a lanthanum atom trapped in the cavity of C_{60}, called endofullerene, $C_{60}La$, was published. (Heath et al., 1985). Another consequent experiment proved the stability of $C_{60}La^+$ against H_2, O_2, NO, and NH_3. (Weiss et al., 1988). This suggested that the lanthanum atom can be "protected" by being encapsulated in the fullerene. Since then, a number of studies focusing on novel properties of C_{60} and its interactions with other species have been carried out. (Ruoff et al., 1993; Diederich and Gómez-López, 1999; Bakry et al., 2007; Mignolet et al., 2013; Wang et al., 2014; Elliott et al., 2018; Kouřil et al., 2018) Some investigations concentrated on medical applications, hydrogen storage, and various endofullerene. (Wang et al., 2013; Srivastava et al., 2016; Srivastava et al., 2017; Elliott et al., 2018; Kouřil et al., 2018). Due to the fullerene's unique cage-like cavity, a procedure called molecular surgery can be performed to entrap an atom or molecule. (Murata et al., 2006; Krachmalnicoff et al., 2016). Utilizing this technique, encapsulation of molecular hydrogen and HF were successfully achieved. (Murata et al., 2006; Krachmalnicoff et al., 2016). In addition, a recent paper by Jana and Chattaraj (2020) describes the effects of a molecular reaction environment, dodecahedrane, on the He dimer bonding. Also, theoretical studies of a new type of endofullerenes with superalkali have been performed. (Srivastava et al., 2016; Srivastava et al., 2017) Superalkalis are clusters with very low adiabatic ionization energies. (Gutsev and Boldyrev, 1982; Gutsev and Boldyrev, 1983; Gutsev and Boldyrev, 1987; Lia et al., 1988; Gutsev and Boldyrev, 1990;

Tong et al., 2013a; Tong et al., 2013b). The first and most common superalkalis have the formula $M_{k+1}L$, where M is an alkali atom with valence k and L is an electronegative atom. (Gutsev and Boldyrev, 1985; Gutsev and Boldyrev, 1987; Zhao et al., 2017). Nambiar et al. (2021) showed the importance of these compounds through a density functional computational study to improve the efficacy of redox reactions.

The concentration of carbon dioxide (CO_2) in the atmosphere has been increasing constantly since the early 20th century with rapid industrialization. (D'Amato and Akdis, 2020; Kuzovkin and Semenov, 2020). This is a globally recognized issue as CO_2 contributes significantly to the greenhouse effect and the acidification of the oceans. (Crowley and Berner, 2001; Hönisch et al., 2012). Increment of atmospheric temperature causes climate change that threatens the overall ecosystem. To capture CO_2 molecules present in the air, various methods have been employed such as packed column of monoethanolamine and metal-organic frameworks. (Lv et al., 2015; Li et al., 2019; Li et al., 2020). The next step is activating CO_2 molecules and converting them to value-added chemicals such as hydrocarbon fuels. (Hu et al., 2013). The activation of CO_2 is extremely complex due to its stability and much efforts have been made by researchers to directly convert it into liquid hydrocarbons, useful for the aviation sector as novel jet fuels (Boreriboon et al., 2018; Vogt et al., 2019; Yao et al., 2020) or into oxygenates, such as ethanol. (Song et al., 2016; Bai et al., 2017; Wang et al., 2018). This conversion, whether it involves a direct CO_2 hydrogenation route or not, entails the usage of metal-based catalysts to ensure an overall reasonable efficiency. (Yao et al., 2020).

In our previous studies, successful activation of CO_2 with a superalkali species, Li_3F_2, were presented. (Park and Meloni, 2017). The computational study showed charge transfer from Li_3F_2 to CO_2, which indicates migration of the unpaired electron from Li_3F_2 to CO_2. The activated CO_2 showed geometric change such as bent $\widehat{OCO}$ angle. The activated CO_2 then can be transformed to other organic molecules with catalysis. (Liu et al., 2016; Luc et al., 2017). Removing the unpaired electron from $[Li_3F_2{\cdot}CO_2]$ cluster weakens the interaction between Li_3F_2 and CO_2 and geometry of CO_2 returns back to the linear form. (Park and Meloni, 2017). The superalkali Li_3F_2 was observed and characterized experimentally. (Yokoyama et al., 2000; Haketa et al., 2002). They also confirmed three stable Li_3F_2 structures through a computational density functional approach. (Haketa et al., 2002). In this investigation, the Li_3F_2-doped fullerene and its endo-reaction with CO_2 has been characterized using the B3LYP/6-31G* level of theory. These results are explained in terms of energetics and molecular orbitals of the species involved. In addition, these findings will be beneficial in providing insights for CO_2 reduction and in helping the exploration of new materials with tailored properties.

Computational Methods

Geometries and total electronic energies of the investigated species were calculated at the B3LYP/6-31G* level of theory (Becke, 1988; Lee et al., 1988) using the computational software Gaussian09. (Frisch et al., 2016). B3LYP is one of the most commonly used density functional theory (DFT) methods that employs a three-parameter exchange functional developed by Becke (1992) and Becke (1993) with a correlational functional proposed by Lee, Yang, and Parr (LYP) Becke (1988) to approximate the exchange-correlation energy. The B3LYP/6-31G* level has been employed to study endofullerene systems because it yields reliable geometries and energies. (Wang et al., 2013; Srivastava et al., 2016; Srivastava et al., 2017). Partial atomic charges are calculated based on the Mulliken population analysis (Mulliken, 1955) and natural bond orbital (NBO) population analysis. (Reed et al., 1985).

The adiabatic ionization energy (AIE) is calculated by taking the zero-point energy corrected electronic energy difference between the optimized neutral and cation, whereas the adiabatic electron affinity (AEA) is obtained by subtracting the zero-point-energy corrected electronic energy of the optimized anion and neutral. All the optimized structures have real vibrational frequencies and their Cartesian coordinates have been reported in the **Supplementary Material**.

RESULTS AND DISCUSSION

The main intent of this computational investigation is to study the interactions relevant to the reduction of CO_2 by the superalkali Li_3F_2 inside our molecular reaction vessel, i.e., C_{60}, and see how this environment affects the CO_2 activation. The system is fairly large and, therefore, computationally challenging to investigate. We have analyzed the possible interactions between the fullerene and the two reactants, CO_2 and Li_3F_2. All the computed energetics are reported in **Table 1** together with the available literature (experimental and computed) values.

Figure 1 reports the optimized geometries for CO_2 and CO_2^-, $Li_3F_2(C_{2v})$, $Li_3F_2(D_{3h})$ and their cations. The structures of CO_2 and CO_2^- reproduce well the literature experimental values for both bond distances and bond angles. In fact, for CO_2 we have $r_{C\text{-}O}$ = 1.17 Å (1.16 Å) (Herzberg, 1966) and for CO_2^- we have $r_{C\text{-}O}$ = 1.25 Å (1.25 Å) (Hartman and Hisatsune, 1966) and ∠OCO° = 134° (127 ± 7°) . (Hartman and Hisatsune, 1966). Both the geometries of the lowest energy $Li_3F_2(C_{2v})$ isomer, trigonal bipyramidal $Li_3F_2(D_{3h})$, and their cations are in agreement with our previous work. (Park and Meloni, 2017; Cochran and Meloni, 2014). **Figure 2** shows the two superalkali isomers reducing the CO_2. The geometry for the previously studied C_{2v} isomer interacting with CO_2 is in agreement with our previous results, (Park and Meloni, 2017), whereas the $D_{3h}{\cdot}CO_2$ species is reported for the first time. When the D_{3h} structure reacts with CO_2, the trigonal bipyramidal geometry is distorted by increasing two "equatorial" Li-Li distances, maintaining only the Li(1)-Li(2) distance of 2.30 Å, with Li(3) being closer to the CO_2, Li(3)-O(7) = Li(3)-O(8) = 2.03 Å and increasing the axial F-F distance from 2.40 to 2.68 Å. The ∠OCO° bond angle is 128° and the C-O bond length is 1.26 Å. The Li_3F_2 isomers have similar binding energy with CO_2, with the C_{2v} isomer

TABLE 1 | Energetics of all the species relevant to this study calculated at the B3LYP/6-31G* level of theory. The zero-point-energy corrected total electronic energy (E_0) is in Hartree, the adiabatic ionization energy (AIE) and adiabatic electron affinity are in eV, and the binding energy at 0 K is in kJ mol^{-1}. [SA·CO_2] stays for the endo superalkali·CO_2 complex.

Species	E_0	AIE	AIE liter	AEA	AEA liter	BE	BE liter
CO_2	−188.569349	13.6	13.78 Herzberg (1966)	−1.27	−0.60 Wang et al. (1988) −1.60 de Vries et al. (1992)	–	–
$Li_3F_2(C_{2v})$	−222.473494	3.91	3.80 Hartman and Hisatsune (1966)	0.63	0.59 Hartman and Hisatsune (1966)	–	–
$Li_3F_2(D_{3h})$	−222.459703	4.24	3.86 Hartman and Hisatsune (1966)	0.36	0.75 Hartman and Hisatsune (1966)	–	–
C_{60}	−2285.799198	7.08	7.54 Sikorska and Gaston (2020)	2.25	2.68 Knapp et al. (1986)	–	–
$Li_3F_2(C_{2v})·CO_2$	−411.112817	5.42	5.21 Park and Meloni, (2017)	0.97	0.36 Park and Meloni (2017)	184	163 Park and Meloni (2017)
$Li_3F_2(D_{3h})·CO_2$	−411.096882	5.25	–	0.80	–	178	–
$C_{60}·CO_2$	−2474.312373	7.08	–	2.27	–	−147[a]	–
$C_{60}·Li_3F_2(D_{3h})$	−2508.304346	5.64	–	2.45	–	119[a]	–
$C_{60}·[SA·CO_2]$	−2696.601627	5.73	–	2.56	–	[a]	–

[a]*This binding energy at 0 K corresponds to the negative solvation energy at 0 K that C_{60} exerts on the encapsulated species, reactants, Li_3F_2 and CO_2, and product SA·CO_2 (see text).*

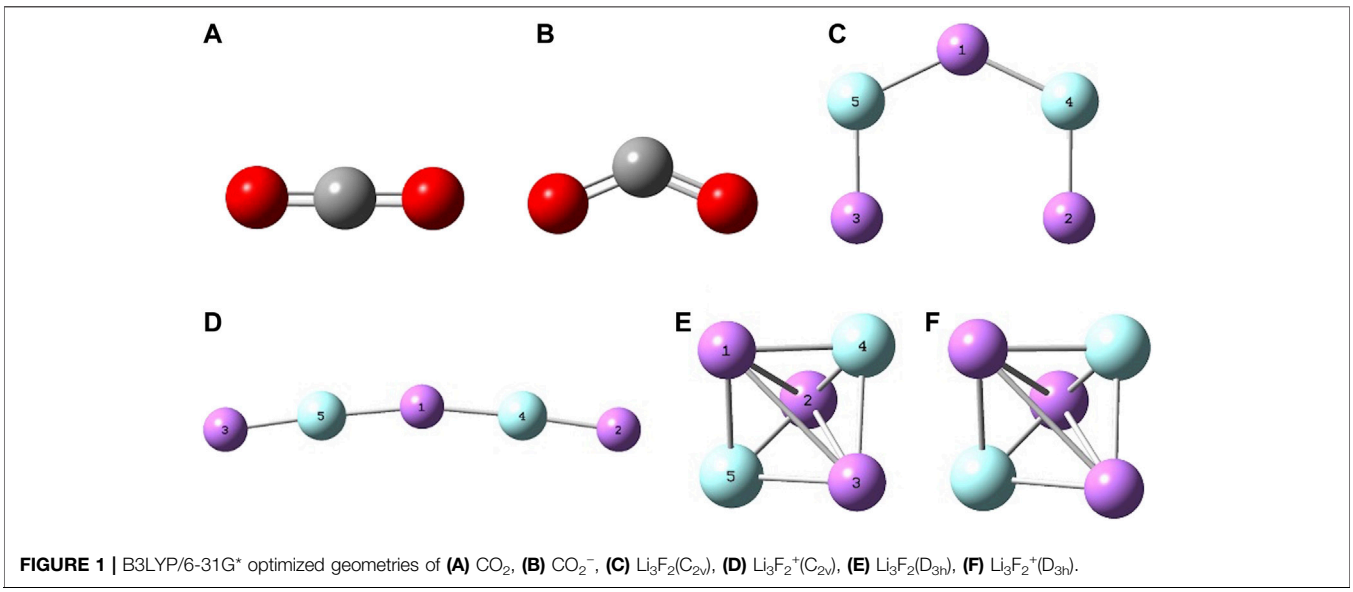

FIGURE 1 | B3LYP/6-31G* optimized geometries of **(A)** CO_2, **(B)** CO_2^-, **(C)** $Li_3F_2(C_{2v})$, **(D)** $Li_3F_2^+(C_{2v})$, **(E)** $Li_3F_2(D_{3h})$, **(F)** $Li_3F_2^+(D_{3h})$.

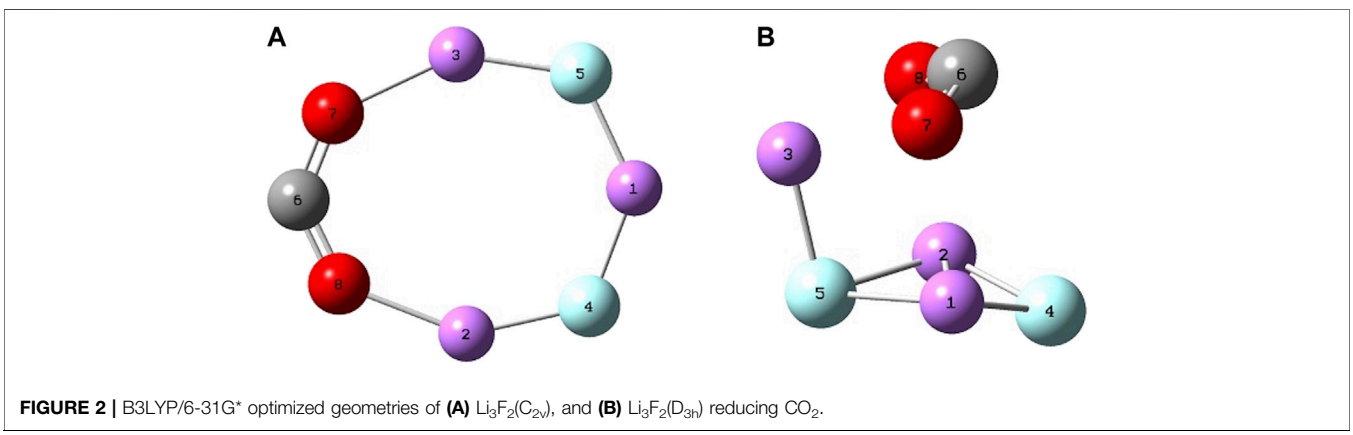

FIGURE 2 | B3LYP/6-31G* optimized geometries of **(A)** $Li_3F_2(C_{2v})$, and **(B)** $Li_3F_2(D_{3h})$ reducing CO_2.

presenting a stronger interaction of 184 kJ mol^{-1}. These clusters can be defined as "free" or "naked" because they are isolated in the gas phase. The presented energy values are calculated at the B3LYP/6-31G* level and are within 10% from the literature reported quantities, whether they are experimental or computed at very high level of theory.

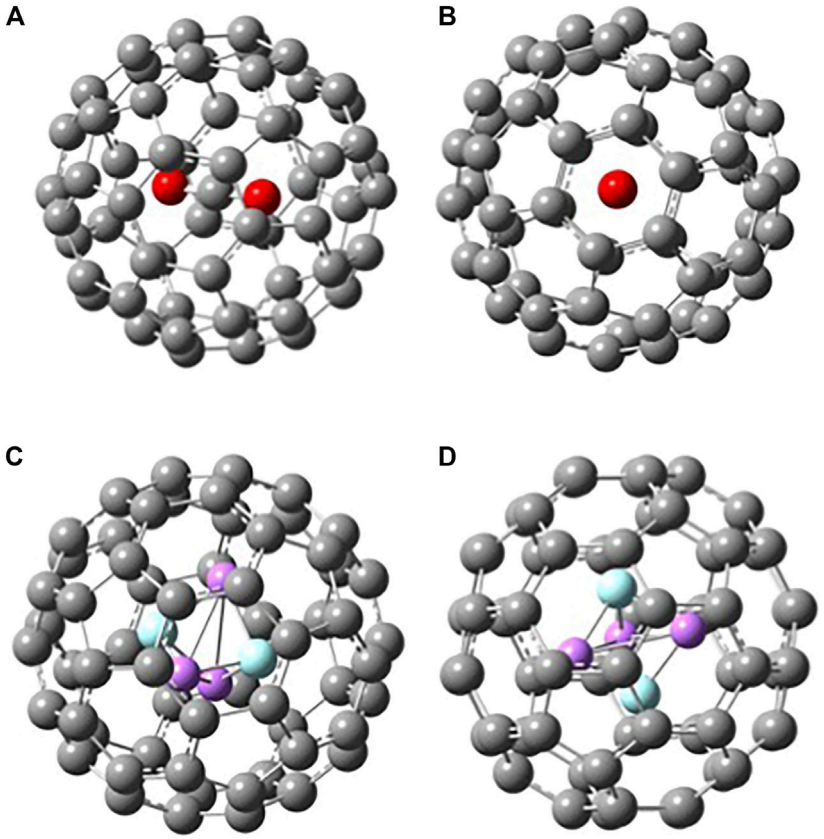

FIGURE 3 | Two different views of B3LYP/6-31G* optimized structures of **(A)**-**(B)** $C_{60} \cdot CO_2$ and **(C)**-**(D)** $C_{60} \cdot Li_3F_2(D_{3h})$.

When a molecule is inserted in the fullerene (yielding an endofullerene), the chemical system is not free, but it will be subjected to the interactions with the carbon cage ("solvation effects"). In **Figure 3**, the two endofullerenes with CO_2 and Li_3F_2 are shown. In the case of carbon dioxide, it is clear from the energetics presented in **Table 1** that CO_2 is destabilized by C_{60} having a negative binding energy at 0 K of −147 kJ mol^{-1} or a solvation energy at 0 K of 147 kJ mol^{-1}, calculated as $E_0(CO_2) + E_0(C_{60})—E_0(C_{60}{\cdot}CO_2)$. The CO_2 occupies the center of the C_{60}, aligned with the C_3 axis passing through a hexagonal face, minimizing its interactions with the C cage. The solvation energy is more properly defined as the Gibbs free energy change associated with the transfer of a molecule from the gas phase into a solvent, i.e., it provides the relative equilibrium populations of a species between gas phase and the solvent. Therefore, we should also know the entropy change connected with this process. The values that we are reporting in this investigation are at 0 K, so that $\Delta_{solv}H_0^o = \Delta_{solv}G_0^o = -\,\mathrm{BE}\,(\mathrm{solvent} - \mathrm{species})$, from which we can see that negative binding energies correspond to positive solvation energies (destabilizing effect). For the encapsulated superalkali two main findings can be noticed. First, the superalkali inside the fullerene is "forced" to assume a D_{3h}

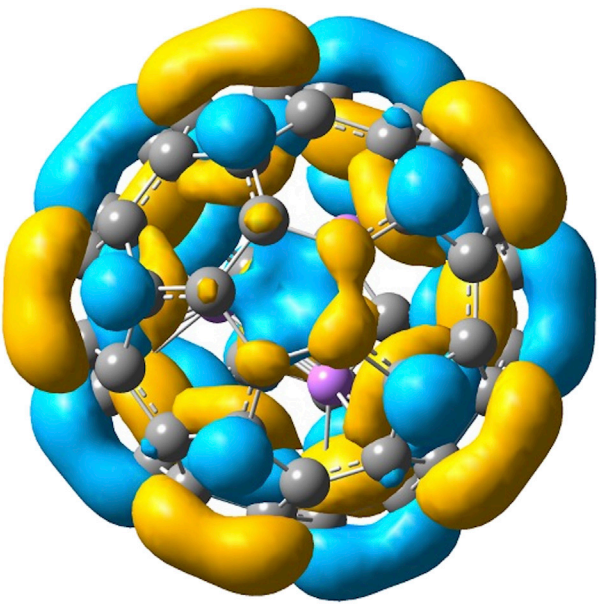

FIGURE 4 | HOMO of $C_{60} \cdot Li_3F_2(D_{3h})$.

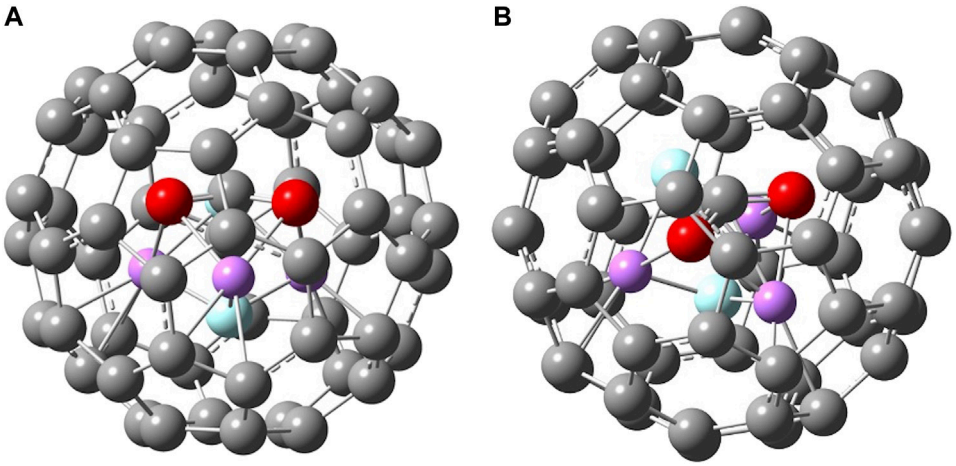

FIGURE 5 | Two different views of B3LYP/6-31G* optimized geometry of $C_{60} \cdot Li_3F_2(D_{3h}) \cdot CO_2$.

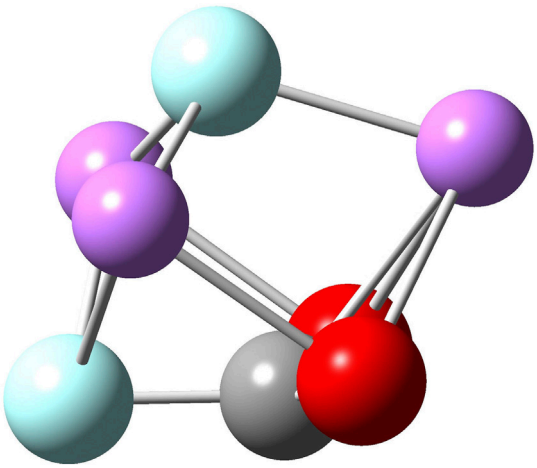

FIGURE 6 | B3LYP/6-31G* optimized geometry of the $Li_3F_2{\cdot}CO_2$ complex inside C_{60}.

geometry, a structure almost identical to the free D_{3h} cluster but less stable than the free C_{2v} cluster. Despite having started the Li_3F_2 geometry optimization from different initial configurations, the optimized structure inside the fullerene resulted in the trigonal bipyramidal geometry. The Li-F distances are shortened in C_{60} from 1.83 (free superalkali) to 1.77 Å, which corresponds to a compression along the F-F distance from 2.40 to 2.21 Å, and the two Li-Li bonds elongate to 2.40 Å. The second result is that C_{60} interacts strongly with Li_3F_2 with a binding energy at 0 K of 119 kJ mol^{-1} or solvation energy at 0 K of −119 kJ mol^{-1}, calculated as $E_0(Li_3F_2(D_{3h}))$ + $E_0(C_{60})$—$E_0(C_{60}{\cdot}Li_3F_2(D_{3h}))$. This interaction is not a reduction of C_{60}, where the electron from the superalkali is transferred to the fullerene. In fact, upon ionization of $C_{60}{\cdot}Li_3F_2$, the encapsulated Li_3F_2 retains its trigonal bipyramidal structure, just slightly distorted (as described above) due to the interactions with C_{60}. In addition, looking at the Mulliken population and the natural orbital population neither the endo-$Li_3F_2(D_{3h})$ nor the C_{60} show an increase or change of electron charges. The $C_{60}{\cdot}Li_3F_2$ HOMO, the main contribution of which is given by C 2p AO's, is delocalized almost entirely on the fullerene (**Figure 4**). The fact that the $C_{60}{\cdot}Li_3F_2$ AIE is much lower than C_{60} AIE, 5.64 vs. 7.08 eV, respectively, can be explained using a molecular orbital character argument. The interaction of C_{60} with the superalkali makes the HOMO of fullerene less bonding, and consequently, most of the C-C bonds are elongated by 0.1–0.2 Å. Upon ionization, the C-C bonds in $C_{60}{\cdot}Li_3F_2$ are shortened on average by 0.1 Å, which can be interpreted as the removal of an electron from a HOMO with antibonding character.

The insertion of CO_2 within $C_{60}{\cdot}Li_3F_2(D_{3h})$ produces an unexpected result (**Figure 5**). In previous computational studies, (Zhao et al., 2017; Park and Meloni, 2017; Sikorska and Gaston, 2020), naked superalkali have been shown to be capable of reducing carbon dioxide by transferring an electron and yielding an activated bent CO_2^-. In this investigation, we show that our molecular vessel C_{60} forces the reaction to proceed in a different way (**Figure 6**). From an analysis of the optimized geometries inside fullerene, it is clear that CO_2 is activated by showing a ∠OCO° bond angle of 132° and C-O bond lengths of 1.20 Å, 0.03 Å longer than $r_{C\text{-}O}$ in CO_2 but 0.06 Å shorter than $r_{C\text{-}O}$ in the free $Li_3F_2(D_{3h}){\cdot}CO_2$ species. The activation of CO_2 is achieved by a F transfer from Li_3F_2 to CO_2 with the formation of a C-F bond of 1.38 Å, almost identical to the $r_{C\text{-}F}$ of 1.382 Å in CH_3F. (Demaison et al., 1999). This moiety FCO_2 does not resemble either the fluorocarboxyl radical FCO_2 for which $r_{C\text{-}O}$ is 1.234 Å, $r_{C\text{-}F}$ is 1.310 Å, and ∠OCO° bond angle is 118.8°, (Zelinger et al., 2003), or the fluoroformate ion FCO_2^- for which $r_{C\text{-}O}$ is 1.234 Å, $r_{C\text{-}F}$ is 1.46 Å, and ∠OCO° bond angle is 135.9°. (Arnold et al., 1995; Thomas et al., 2018). In addition, both fluorocarboxyl radical and fluoroformate ion are planar, whereas the endo-reaction species (**Figure 6**) resembles a non-planar

(trigonal pyramidal) FCO_2 that interacts with what it looks like a FLi_3 species. All the attempts to optimize this structure outside C_{60} as free endo-$Li_3F_2{\cdot}CO_2$ returned a $Li_3F_2(D_{3h}){\cdot}CO_2$ geometry. Unfortunately, this prevents us from quantifying the interaction of $Li_3F_2(D_{3h})$ with CO_2 inside C_{60}. In fact, the reaction we need is

$$C_{60} \cdot [SA \cdot CO_2] + C_{60} \rightarrow C_{60} \cdot Li_3F_2(D_{3h}) + C_{60} \cdot CO_2 \quad (1)$$

from which the interaction of $Li_3F_2(D_{3h})$ with CO_2 can be derived if we were able to find the $[SA{\cdot}CO_2]$ reaction product as a free species and then its binding energy (or negative solvation energy) with C_{60}, i.e.,

$$C_{60} \cdot [SA \cdot CO_2] \rightarrow C_{60} + [SA \cdot CO_2] \quad (2)$$

In fact, the interaction of $Li_3F_2(D_{3h})$ with CO_2 inside fullerene can be calculated as:

$$\Delta_r H^o(1) - BE(C_{60} \cdot CO_2) - BE(C_{60} \cdot Li_2F_3(D_{3h})) + BE(C_{60} \cdot [SA \cdot CO_2]) \quad (3)$$

In other words, this expression tells us that the interaction between endo-$Li_3F_2(D_{3h})$ and endo-CO_2, i.e., the BE of superalkali-CO_2 in fullerene, is equal to the enthalpy of reaction (1) plus the solvation energies of CO_2 and $Li_3F_2(D_{3h})$ minus the solvation energy of $[SA{\cdot}CO_2]$. Because we cannot derive this last solvation energy absolute value due to the impossibility of optimizing the free endo-$[SA{\cdot}CO_2]$ species, we can estimate this interaction by performing a single-point energy calculation of the free $[SA{\cdot}CO_2]$ optimized inside C_{60}. This structure necessarily represents a higher energy structure than a real minimum and, therefore, the estimated BE of superalkali-CO_2 in fullerene would denote an upper bound providing us some insights on this interaction. From this computation we get an upper bound for $BE(C_{60} \cdot [SA \cdot CO_2])$ of $-965\ kJ\ mol^{-1}$, which tells us that this endo-product is highly destabilized by C_{60}!

CONCLUSION

The activation of CO_2 by the Li_3F_2 superalkali within C_{60} has been investigated at the B3LYP/6-31G* level of theory. C_{60} has been utilized as a reaction vessel and its interaction with the reactants, superalkali and carbon dioxide, have been computed. C_{60} is capable of forcing a superalkali geometry, which does not present the global minimum in the gas phase. Specifically, Li_3F_2 takes the D_{3h} structure. C_{60} has a stabilizing effect on the superalkali but a destabilizing effect on the CO_2, as it can be deduced by the binding energies of these two systems, $BE(C_{60}{\cdot}CO_2) = -147\ kJ\ mol^{-1}$ and $BE(C_{60}{\cdot}Li_3F_2) = 119\ kJ\ mol^{-1}$. Upon interaction of $Li_3F_2(D_{3h})$ with CO_2 inside fullerene, CO_2 is clearly activated showing a $\angle OCO^{\circ}$ bond angle of 132° and C-O bond lengths of 1.20 Å, 0.03 Å longer than $r_{C\text{-}O}$ in CO_2 but 0.06 Å shorter than $r_{C\text{-}O}$ in the free $Li_3F_2(D_{3h}){\cdot}CO_2$ species. The activation of CO_2 is achieved by a F transfer from Li_3F_2 to CO_2 with the formation of a C-F bond of 1.38 Å. Due to the impossibility of optimizing a free superalkali-CO_2 complex, $[SA{\cdot}CO_2]$, resembling the one optimized within the C_{60}, a single-point energy calculation has been performed on the free $[SA{\cdot}CO_2]$. This energy has been utilized to provide an upper bound for the binding energy of $Li_3F_2(D_{3h})$ with CO_2 within C_{60} of $-965\ kJ\ mol^{-1}$, showing that C_{60} destabilizes the reaction product.

DATA AVAILABILITY STATEMENT

The original contribution presented in the study are included in the article/**Supplementary Material**, further inquiries can be directed to the corresponding author.

AUTHOR CONTRIBUTIONS

All authors listed have made a substantial, direct, and intellectual contribution to the work and approved it for publication.

FUNDING

This research was supported by the American Chemical Society Petroleum Research under the fund grant number #56067-UR6.

SUPPLEMENTARY MATERIAL

The Supplementary Material for this article can be found online at: https://www.frontiersin.org/articles/10.3389/fchem.2021.712960/full#supplementary-material

REFERENCES

Arnold, D. W., Bradforth, S. E., Kim, E. H., and Neumark, D. M. (1995). Study of Halogen–Carbon Dioxide Clusters and the Fluoroformyloxyl Radical by Photodetachment of $X^-(CO_2)$ (X=I,Cl,Br) and FCO_2^-. *J. Chem. Phys.* 102 (9), 3493–3509. doi:10.1063/1.468575

Bai, S., Shao, Q., Wang, P., Dai, Q., Wang, X., and Huang, X. (2017). Highly Active and Selective Hydrogenation of CO2 to Ethanol by Ordered Pd–Cu Nanoparticles. *J. Am. Chem. Soc.* 139 (20), 6827–6830. doi:10.1021/jacs.7b03101

Bakry, R., Vallant, R. M., Najam-ul-Haq, M., Rainer, M., Szabo, Z., Huck, C. W., et al. (2007). Medicinal Applications of Fullerenes. *Int. J. Nanomed.* 2 (4), 639–649.

Becke, A. D. (1992). A New Mixing of Hartree-Fock and Local Density-Functional Theories. *J. Chem. Phys.* 98, 1372–1377.

Becke, A. D. (1988). Density-functional Exchange-Energy Approximation with Correct Asymptotic Behavior. *Phys. Rev. A.* 38, 3098–3100. doi:10.1103/physreva.38.3098

Becke, A. D. (1993). Density-functional Thermochemistry. III. The Role of Exact Exchange. *J. Chem. Phys.* 98, 5648–5652. doi:10.1063/1.464913

Boreriboon, N., Jiang, X., Song, C., and Prasassarakich, P. (2018). Higher Hydrocarbons Synthesis from CO_2 Hydrogenation over K- and La-Promoted Fe–Cu/TiO_2 Catalysts. *Top. Catal.* 61 (15), 1551–1562. doi:10.1007/s11244-018-1023-1

Cochran, E., and Meloni, G. (2014). Hypervalence in Monoxides and Dioxides of Superalkali Clusters. *J. Chem. Phys.* 140, 204319. doi:10.1063/1.4879658

Crowley, T. J., and Berner, R. A. (2001). CO2 and Climate Change. *Science* 292870 (5518).

D'Amato, G., and Akdis, C. A. (2020). Global Warming, Climate Change, Air Pollution and Allergies. *Allergy* 75 (9), 2158–2160.

de Vries, J., Steger, H., Kamke, B., Menzel, C., Weisser, B., Kamke, W., et al. (1992). Single-photon Ionization of C_{60}^- and C_{70}^-Fullerene with Synchrotron Radiation: Determination of the Ionization Potential of C_{60}. *Chem. Phys. Lett.* 188 (3), 159–162. doi:10.1016/0009-2614(92)90001-4

Demaison, J., Breidung, J., Thiel, W., and Papousek, D. (1999). The Equilibrium Structure of Methyl Fluoride. *Struct. Chem.* 10 (2), 129–133. doi:10.1023/a:1022085314343

Diederich, F., and Gómez-López, M. (1999). Supramolecular Fullerene Chemistry. *Chem. Soc. Rev.* 28, 263–277. doi:10.1039/a804248i

Elliott, S. J., Bengs, C., Kouril, K., Meier, B., Alom, S., Whitby, R. J., et al. (2018). NMR Lineshapes and Scalar Relaxation of the Water-Endofullerene $H_2{}^{17}O@C_{60}$. *ChemPhysChem* 19, 251–255. doi:10.1002/cphc.201701330

Frisch, M. J., Trucks, G. W., Schlegel, H. B., Scuseria, G. E., Robb, M. A., Cheeseman, J. R., et al. (2016). Gaussian 09., *Revision A.02*. Wallingford, CT.: Gaussian. Inc.

Gutsev, G. L., and Boldyrev, A. I. (1983). An Explanation of the High Electron Affinities of the 5d-Metal Hexafluorides. *Chem. Phys. Lett.* 101, 441–445. doi:10.1016/0009-2614(83)87510-1

Gutsev, G. L., and Boldyrev, A. I. (1982). DVM Xα Calculations on the Electronic Structure of "Superalkali" Cations. *Chem. Phy. Lett.* 92, 262–266. doi:10.1016/0009-2614(82)80272-8

Gutsev, G. L., and Boldyrev, A. I. (1987). The Electronic Structure of Superhalogens and Superalkalies. *Russ. Chem. Rev.* 56, 519–531. doi:10.1070/rc1987v056n06abeh003287

Gutsev, G. L., and Boldyrev, A. I. (1985). The Theoretical Investigation of the Electron Affinity of Chemical Compounds. *Adv. Chem. Phys.* 61, 169–221.

Gutsev, G. L., and Boldyrev, A. I. (1990). Theoretical Estimation of the Maximal Value of the First, Second and Higher Electron Affinity of Chemical Compounds. *J. Phys. Chem.* 94, 2256–2259. doi:10.1021/j100369a012

Haketa, N., Yokoyama, K., Tanaka, H., and Kudo, H. (2002). Theoretical Study on the Geometric and Electronic Structure of the Lithium-Rich $Li_nF_{(n-1)}$ (N=2-5) Clusters. *J. Mol. Struct. THEOCHEM.* 577, 55–67. doi:10.1016/s0166-1280(01)00655-8

Hartman, K. O., and Hisatsune, I. C. (1966). Infrared Spectrum of Carbon Dioxide Anion Radical. *J. Chem. Phys.* 44 (5), 1913–1918. doi:10.1063/1.1726961

Heath, J. R., O'Brien, S. C., Zhang, Q., Liu, Y., Curl, R. F., Tittel, F. K., et al. (1985). Lanthanum Complexes of Speroidal Carbon Shells. *J. Am. Chem. Soc.* 107, 7779–7780. doi:10.1021/ja00311a102

Herzberg, G. (1966). *Electronic Spectra and Electronic Structure of Polyatomic Molecules*. New York: Van Nostrand.

Hönisch, B., Ridgwell, A., Schmidt, D. N., Thomas, E., Gibbs, S. J., Sluijs, A., et al. (2012). The Geological Record of Ocean Acidification. *Science* 335 (6072), 1058–1063. doi:10.1126/science.1208277

Hu, B., Guild, C., and Suib, S. L. (2013). Thermal, Electrochemical, and Photochemical Conversion of CO_2 to Fuels and Value-Added Products. J. Co_2 Util. 1, 18–27. doi:10.1016/j.jcou.2013.03.004

Jana, G., and Chattaraj, P. K. (2020). Effect of Substitution on the Bonding in He Dimer Confined within Dodecahedrane: A Computational Study. *J. Comput. Chem.* 41, 2398–2405. doi:10.1002/jcc.26403

Knapp, M., Echt, O., Kreisle, D., Märk, T. D., and Recknagel, E. (1986). Formation of long-lived CO_2^-, N_2O^-, and their dimer anions, by electron attachment to van der waals clusters. *Chem. Phys. Lett.* 126 (3), 225–231. doi:10.1016/s0009-2614(86)80074-4

Kouřil, K., Meier, B., Alom, S., Whitby, R. J., and Levitt, M. H. (2018). Alignment of ^{17}O-Enriched Water–Endofullerene $H_2O@C_{60}$ in a Liquid crystal Matrix. *Faraday Discuss.* 212, 517–532. doi:10.1039/c8fd00095f

Krachmalnicoff, A., Bounds, R., Mamone, S., Alom, S., Concistrè, M., Meier, B., et al. (2016). The Dipolar Endofullerene $HF@C_{60}$. *Nat. Chem.* 8, 953–957. doi:10.1038/nchem.2563

Kroto, H. W., Heath, J. R., O'Brien, S. C., Curl, R. F., and Smalley, R. E. (1985). C_{60} : Buckminsterfullerene. *Nature* 318, 162–163. doi:10.1038/318162a0

Kuzovkin, V. V., and Semenov, S. M. (2020). Growth Rate of Carbon Dioxide Concentration in the Atmospheric Surface Layer in the Late 20th Century and Early 21st Century. *Russ. Meteorol. Hydrol.* 45 (3), 207–210. doi:10.3103/s1068373920030097

Lee, C., Yang, W., and Parr, R. G. (1988). Development of the Colle-Salvetti Correlation-Energy Formula into a Functional of the Electron Density. *Phys. Rev. B* 37, 785–789. doi:10.1103/physrevb.37.785

Li, K., Feron, P. H. M., Jones, T. W., Jiang, K., Bennett, R. D., and Hollenkamp, A. F. (2020). Energy Harvesting from Amine-Based CO2 Capture: Proof-Of-Concept Based on Mono-Ethanolamine. *Fuel* 263, 116661. doi:10.1016/j.fuel.2019.116661

Li, Z., Wang, L., Li, C., Cui, Y., Li, S., Yang, G., et al. (2019). Absorption of Carbon Dioxide Using Ethanolamine-Based Deep Eutectic Solvents. *ACS Sustain. Chem. Eng.* 7 (12), 10403–10414. doi:10.1021/acssuschemeng.9b00555

Lia, S. G., Bartmess, J. E., Liebman, J. F., Homes, J. L., Levin, R. D., and Mallard, W. G., Gas-Phase Ion and Neutral Thermochemistry. *J. Phys. Chem. Ref. Data*, Suppl, 1. 1988, 17, 1–861.

Liu, X., Song, Y., Geng, W., Li, H., Xiao, L., and Wu, W. (2016). Cu-Mo2C/MCM-41: An Efficient Catalyst for the Selective Synthesis of Methanol from CO_2. *Catalysts* 6 (5). doi:10.3390/catal6050075

Luc, W., Collins, C., Wang, S., Xin, H., He, K., Kang, Y., et al. (2017). Ag–Sn Bimetallic Catalyst with a Core–Shell Structure for CO2 Reduction. *J. Am. Chem. Soc.* 139 (5), 1885–1893. doi:10.1021/jacs.6b10435

Lv, B., Guo, B., Zhou, Z., and Jing, G. (2015). Mechanisms of CO_2 Capture into Monoethanolamine Solution with Different CO_2 Loading during the Absorption/Desorption Processes. *Environ. Sci. Technol.* 49 (17), 10728–10735. doi:10.1021/acs.est.5b02356

Mignolet, B., Johansson, J. O., Campbell, E. E. B., and Remacle, F. (2013). Probing Rapidly-Ionizing Super-atom Molecular Orbitals in C_{60} : A Computational and Femtosecond Photoelectron Spectroscopy Study. *ChemPhysChem* 14, 3332–3340. doi:10.1002/cphc.201300585

Mulliken, R. S. (1955). Electronic Population Analysis on LCAO-MO Molecular Wave Functions. I. *J. Chem. Phys.* 23 (10), 1833–1840. doi:10.1063/1.1740588

Murata, M., Murata, Y., and Komatsu, K. (2006). Synthesis and Properties of Endohedral C_{60} Encapsulating Molecular Hydrogen. *J. Am. Chem. Soc.* 128, 8024–8033. doi:10.1021/ja061857k

Nambiar, S. R., Jana, G., and Chattaraj, P. K. (2021). Can Superalkalis and Superhalogens Improve the Efficacy of. Redox Reactions? *Chem. Phys. Lett.* 762, 138131. doi:10.1016/j.cplett.2020.138131

Park, H., and Meloni, G. (2017). Reduction of Carbon Dioxide with a Superalkali. *Dalton Trans.* 46, 11942–11949. doi:10.1039/c7dt02331f

Reed, A. E., Weinstock, R. B., and Weinhold, F. (1985). Natural Population Analysis. *J. Chem. Phys.* 83, 735–746. doi:10.1063/1.449486

Ruoff, R. S., Tse, D. S., Malhotra, R., and Lorents, D. C. (1993). Solubility of C_{60} in a Variety of Solvents. *J. Phys. Chem.* 97, 3379–3383. doi:10.1021/j100115a049

Sikorska, C., and Gaston, N. (2020). N4Mg6M (M = Li, Na, K) Superalkalis for CO2 Activation. *J. Chem. Phys.* 153 (14), 144301. doi:10.1063/5.0025545

Song, Y., Peng, R., Hensley, D. K., Bonnesen, P. V., Liang, L., Wu, Z., et al. (2016). High-Selectivity Electrochemical Conversion of CO_2 to Ethanol Using a Copper Nanoparticle/N-Doped Graphene Electrode. *ChemistrySelect* 1 (19), 6055–6061. doi:10.1002/slct.201601169

Srivastava, A. K., Kumar, A., and Misra, N. (2017). Superalkali@C_{60}-superhalogen: Structure and Nonlinear Optical Properties of a New Class of Endofullerene Complexes. *Chem. Phys. Lett.* 682, 20–25. doi:10.1016/j.cplett.2017.05.070

Srivastava, A. K., Pandey, S. K., and Misra, N. (2016). Prediction of superalkali@C_{60} Endofullerenes, Their Enhanced Stability and Interesting Properties. *Chem. Phys. Lett.* 655-656, 71–75. doi:10.1016/j.cplett.2016.05.039

Thomas, D. A., Mucha, E., Gewinner, S., Schöllkopf, W., Meijer, G., and von Helden, G. (2018). Vibrational Spectroscopy of Fluoroformate, FCO_2^-, Trapped in Helium Nanodroplets. *J. Phys. Chem. Lett.* 9 (9), 2305–2310. doi:10.1021/acs.jpclett.8b00664

Tong, J., Wu, D., Li, Y., Wang, Y., and Wu, Z. (2013). Superalkali Character of Alkali-Monocyclic (pseudo)Oxocarbon Clusters. *Dalton Trans.* 42, 9982–9989. doi:10.1039/c3dt50224d

Tong, J., Wu, Z., Li, Y., and Wu, D. (2013). Prediction and Characterization of Novel Polynuclear Superalkali Cations. *Dalton Trans.* 42, 577–584. doi:10.1039/c2dt31429k

Vogt, C., Monai, M., Kramer, G. J., and Weckhuysen, B. M. (2019). The Renaissance of the Sabatier Reaction and its Applications on Earth and in Space. *Nat. Catal.* 2 (3), 188–197. doi:10.1038/s41929-019-0244-4

Wang, K., Liu, Z., Wang, X., and Cui, X. (2014). Enhancement of Hydrogen Binding Affinity with Low Ionization Energy Li_2F Coating on C_{60} to Improve Hydrogen Storage Capacity. *Int. J. Hydrog. Energ.* 39, 15639–15645. doi:10.1016/j.ijhydene.2014.07.132

Wang, L.-S., Reutt, J. E., Lee, Y. T., and Shirley, D. A. (1988). High Resolution UV Photoelectron Spectroscopy of CO_2^+, COS^+ and CS_2^+ Using Supersonic

Molecular Beams. *J. Electron. Spectros. Relat. Phenomena* 47, 167–186. doi:10.1016/0368-2048(88)85010-2

Wang, L., Wang, L., Zhang, J., Liu, X., Wang, H., Zhang, W., et al. (2018). Selective Hydrogenation of CO_2 to Ethanol over Cobalt Catalysts. *Angew. Chem. Int. Ed.* 57 (21), 6104–6108. doi:10.1002/anie.201800729

Wang, S.-J., Li, Y., Wang, Y.-F., Wu, D., and Li, Z.-R. (2013). Structures and Nonlinear Optical Properties of the Endohedral Metallofullerene-Superhalogen Compounds Li@C_{60}-BX_4 (X=F, Cl, Br). *Phys. Chem. Chem. Phys.* 15, 12903–12910. doi:10.1039/c3cp51443a

Weiss, F. D., Elkind, J. L., O'Brien, S. C., Curl, R. F., and Smalley, R. E. (1988). Photophysics of Metal Complexes of Spheroidal Carbon Shells. *J. Am. Chem. Soc.* 110, 4464–4465. doi:10.1021/ja00221a085

Yao, B., Xiao, T., Makgae, O. A., Jie, X., Gonzalez-Cortes, S., Guan, S., et al. (2020). Transforming Carbon Dioxide into Jet Fuel Using an Organic Combustion-Synthesized Fe-Mn-K Catalyst. *Nat. Commun.* 11 (1), 6395. doi:10.1038/s41467-020-20214-z

Yokoyama, K., Haketa, N., Tanaka, H., Furukawa, K., and Kudo, H. (2000). Ionization Energies of Hyperlithiated Li_3F Molecule and $Li_nF_{(n-1)}$ (N=3, 4) Clusters. *Chem.Phys. Lett.* 330, 339–346. doi:10.1016/s0009-2614(00)01109-x

Zelinger, Z., Dréan, P., Walters, A., Moreno, J. R. A., Bogey, M., Pernice, H., et al. (2003). Gas-phase Detection of the FCO_2 Radical by Millimeter Wave and High Resolution Infrared Spectroscopy Assisted by Ab Initio Calculations. *J. Chem. Phys.* 118 (3), 1214–1220. doi:10.1063/1.1528607

Zhao, T., Wang, Q., and Jena, P. (2017). Rational Design of Super-alkalis and Their Role in CO_2 Activation. *Nanoscale* 9, 4891–4897. doi:10.1039/c7nr00227k

Conflict of Interest: The authors declare that the research was conducted in the absence of any commercial or financial relationships that could be construed as a potential conflict of interest.